Nonlocal Convective PBL Model Based on New Third- and Fourth-Order Moments

Y. CHENG

NASA Goddard Institute for Space Studies, New York, New York

V. M. CANUTO

NASA Goddard Institute for Space Studies, and Department of Applied Physics and Mathematics, Columbia University, New York, New York

A. M. HOWARD

NASA Goddard Institute for Space Studies, New York, New York, and Department of Earth, Atmosphere, and Planetary Sciences, MIT, Cambridge, Massachusetts

(Manuscript received 7 July 2004, in final form 19 November 2004)

ABSTRACT

The standard approach to studying the planetary boundary layer (PBL) via turbulence models begins with the first-moment equations for temperature, moisture, and mean velocity. These equations entail second-order moments that are solutions of dynamic equations, which in turn entail third-order moments, and so on. How and where to terminate (close) the moments equations has not been a generally agreed upon procedure and a variety of models differ precisely in the way they terminate the sequence. This can be viewed as a bottom-up approach. In this paper, a top-down procedure is suggested, worked out, and justified, in which a new closure model is proposed for the fourth-order moments (FOMs). The key reason for this consideration is the availability of new aircraft data that provide for the first time the z profile of several FOMs. The new FOM expressions have nonzero cumulants that the model relates to the z integrals of the third-order moments (TOMs), giving rise to a nonlocal model for the FOMs. The new FOM model is based on an analysis of the TOM equations with the aid of large-eddy simulation (LES) data, and is verified by comparison with the aircraft data. Use of the new FOMs in the equations for the TOMs yields a new TOM model, in which the TOMs are damped more realistically than in previous models. Surprisingly, the new FOMs with nonzero cumulants simplify, rather than complicate, the TOM model as compared with the quasi-normal (QN) approximation, since the resulting analytic expressions for the TOMs are considerably simpler than those of previous models and are free of algebraic singularities. The new TOMs are employed in a second-order moment (SOM) model, a numerical simulation of a convective PBL is run, and the resulting mean potential temperature T, the SOMs, and the TOMs are compared with several LES data. As a final consistency check, T, SOMs, and TOMs are substituted from the PBL run back into the FOMs, which are again compared with the aircraft data.

1. Introduction

The search for a reliable turbulence model to describe the planetary boundary layer (PBL) was pioneered by Mellor and Yamada in the early 1970s (Mellor and Yamada 1974). These types of models were able to reproduce many features of geophysical flows, but shortcomings remained, such as the poor parameterizations of the length scale, the pressure correlations, and the third-order moments. The turbulence-based mixing models can be roughly classified into two categories.

The first category is represented by local models, in which the third-order moments (TOMs) in the equations for the Reynolds stresses, heat fluxes, and temperature variance are neglected. The resulting Reynolds stresses and heat fluxes are directly proportional to the local gradients of the mean wind or mean potential temperature. Though progress has been made to improve these models (e.g., Mellor and Yamada 1974, 1982; Cheng and Canuto 1994; Kantha and Clayson 1994; Nakanishi 2001; Cheng et al. 2002), the main success of local models is achieved in neutral and stably stratified flows while in a convective PBL these models' performance is much less satisfactory (Moeng and Wyngaard 1989). The reason is that large eddies, which are the major contributors to the transport processes, cannot be properly represented by local models. When

Corresponding author address: Dr. Y. Cheng, NASA Goddard Institute for Space Studies, 2880 Broadway, New York, NY 10025. E-mail: ycheng@giss.nasa.gov

used in a general circulation model (GCM), local mixing models produce insufficient vertical transport, predicting the maxima of the relative humidity and the cloud cover too close to the surface, contrary to observations (e.g., Holtslag and Boville 1993).

The second category is represented by nonlocal models. Deardorff (1972), Troen and Mahrt (1986), Holtslag and Moeng (1991), and Wyngaard and Weil (1991) proposed semi-empirical nonlocal models for the temperature and scalar fluxes by including heuristic nonlocal terms, also called countergradient terms. Holtslag and Boville (1993), using the schemes of Troen and Mahrt (1986) and Holtslag et al. (1990), showed that the nonlocal models are capable of transporting moisture more efficiently from the surface to higher vertical levels in a global climate model. Schmidt et al. (2005, manuscript submitted to *J. Climate*) employed the nonlocal transport expressions of Holtslag and Moeng (1991) and Moeng and Sullivan (1994) in the Goddard Institute for Space Studies (GISS) climate model and obtained improved vertical structures of the relative humidity and cloud cover.

The physical nature of nonlocality can be deduced from the turbulence equations. Since the dynamic equations for the TOMs require the knowledge of the fourth-order moments (FOMs), the treatment of the latter becomes a key issue. The most common approximation is the quasi-normal approximation, QN (Tatsumi 1957; O'Brien and Francis 1962; Ogura 1962; Zeman and Lumley 1976; André et al. 1976, 1978; Bougeault 1981; Chen and Cotton 1983; Moeng and Randall 1984; Canuto et al. 1994, 2001). However, the QN does not provide sufficient damping for the TOMs and causes the development of negative energy. André et al. (1976) proposed a "clipping approximation" to limit the unphysical growth of the TOMs so as to satisfy the realizability inequalities. Moeng and Randall (1984) supplemented the TOM model of André et al. (1982) with a down-gradient diffusion term, which was first suggested by Deardorff (1978), to damp the spurious oscillations associated with the mean-gradient terms in the TOM equations, but they cautioned that "no theoretical basis exists for choosing the strength of the diffusion coefficient in physical space," and "the model results are sensitive to the choice". While the spurious oscillations appear in the stable region near the top of the PBL, divergences may occur in the unstable region in the low part of the PBL; the algebraic TOM expressions obtained from the stationary equations under the QN exhibit unphysical singularities at moderate buoyancy forcing (see section 4). More recently, Zilitinkevich et al. (1999) and Gryanik and Hartmann (2002) proposed to parameterize the fourth-order cumulants as an expansion in the velocity and temperature skewnesses and solved some of the TOMs from the budget equations.

The present study is motivated by both the shortcomings and the successes of the nonlocal models discussed above. It is our purpose to suggest a new nonlocal PBL model that relies as much as possible on the turbulence dynamic equations rather than on heuristic arguments. Ours is a top-down approach. First, we formulate a new non-Gaussian model for the FOMs. Second, the new FOM model is tested against large eddy simulation (LES) and aircraft data. Third, the new FOMs are substituted in the TOM equations, the stationary solution of which yields a simple algebraic model for the TOMs in terms of the second-order moments (SOMs). Fourth, we substitute the new TOMs in the SOM equations and perform a simulation of a convective PBL. The PBL results are compared with the LES data. Finally, the PBL results are substituted back to the starting FOM model to compare with the aircraft FOM data and by doing so we check the internal consistency of the closure hierarchy. The procedure is illustrated in the following flowchart.

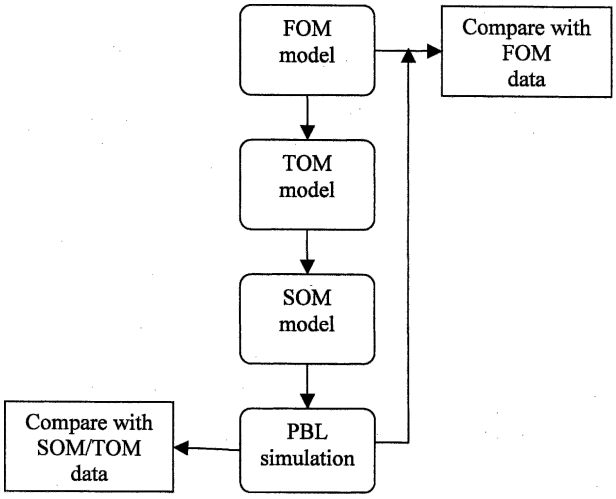

2. SOM equations

To facilitate the discussion, we list the dynamic, second-order closure equations in the convective PBL (see, e.g., Canuto 1992) in appendix A. These equations can be written more explicitly as follows:

Mean field:

$$\frac{\partial T}{\partial t} = -\frac{\partial}{\partial z}\overline{w\theta}. \tag{1}$$

Turbulence fields:

$$\frac{\partial}{\partial t}\overline{w^2} = -\frac{\partial}{\partial z}\overline{w^3} - \frac{2c_4}{\tau_p}\left(\overline{w^2} - \frac{1}{3}\overline{q^2}\right) + \left(2 - \frac{4c_5}{3}\right)g\alpha\overline{w\theta} - \frac{2\varepsilon}{3} \tag{2a}$$

$$\frac{\partial}{\partial t}\overline{u^2} = -\frac{\partial}{\partial z}\overline{u^2 w} - \frac{2c_4}{\tau_p}\left(\overline{u^2} - \frac{1}{3}\overline{q^2}\right) + \frac{2c_5}{3}g\alpha\overline{w\theta} - \frac{2\varepsilon}{3} \tag{2b}$$

$$\frac{\partial}{\partial t}\overline{w\theta} = -\frac{\partial}{\partial z}\overline{w^2\theta} - 2c_6\frac{\overline{w\theta}}{\tau_p} - \overline{w^2}\frac{\partial T}{\partial z} + (1 - c_7)g\alpha\overline{\theta^2} \tag{2c}$$

$$\frac{\partial}{\partial t}\overline{\theta^2} = -\frac{\partial}{\partial z}\overline{w\theta^2} - 4c_2\frac{\overline{\theta^2}}{\tau} - 2\overline{w\theta}\frac{\partial T}{\partial z} \tag{2d}$$

$$\overline{q^2} = \overline{w^2} + 2\overline{u^2}. \tag{2e}$$

Here, T is the mean potential temperature, w and θ are the fluctuating parts of the vertical component of the velocity and the potential temperature, respectively, $\overline{w^2}$ and $\overline{u^2}$ are the vertical and horizontal components of twice the turbulent kinetic energy; $\overline{w\theta}$ is the vertical turbulent heat flux, $\overline{\theta^2}$ is the variance of θ, g is the gravitational acceleration, α is the coefficient of thermal expansion, ε is the dissipation rate, and τ is a dynamic time scale:

$$\tau = \frac{\overline{q^2}}{\varepsilon}. \tag{2f}$$

The parameterizations of ε and τ will be discussed in section 7; τ_p is the return-to-isotropy time scale discussed in appendix A, and the various c's are model constants.

3. TOM equations with modified pressure correlations

To solve Eqs. (2a)–(2d), one needs the TOMs that appear as the first term on the rhs of these equations. The dynamic equations for the TOMs are listed in appendix B, in which we basically follow André et al. (1982) for the closures of the pressure correlations and the dissipation terms, except that we made a modification to the parameterization of the pressure correlation Π_{ij}^{θ} [defined in (B7)]. The new parameterization is

$$\Pi_{ij}^{\theta} = \frac{2c_8}{\tau}\left(\overline{u_i u_j\theta} - \frac{1}{3}\delta_{ij}\overline{u_k u_k\theta}\right) + c_{11}g\alpha(\overline{u_i\theta^2}\delta_{3j} + \overline{u_j\theta^2}\delta_{3i}) - \frac{2c_9}{\tau}\delta_{ij}\overline{u_k u_k\theta}. \tag{3}$$

As discussed in detail in appendix B, the new parameterization (3), being free of the $g\alpha\delta_{ij}w\theta^2$ term, removes a difficulty associated with the widely used closure for Π_{ij}^{θ} that violated the "realizability conservation" described by André et al. (1982).

With the closures for the dissipation and the pressure terms presented in appendix B, the TOM equations read

$$\frac{\partial}{\partial t}\overline{u_i u_j w} = -\frac{\partial}{\partial z}\overline{u_i u_j w^2} + \overline{u_i u_j}\frac{\partial\overline{w^2}}{\partial z} + \overline{u_j w}\frac{\partial\overline{u_i w}}{\partial z} + \overline{u_i w}\frac{\partial\overline{u_j w}}{\partial z} - \frac{2c_8}{\tau}\overline{u_i u_j w} + \lambda(\overline{u_i u_j\theta} + \overline{u_i w\theta}\delta_{3j} + \overline{u_j w\theta}\delta_{3i}), \tag{4a}$$

$$\frac{\partial}{\partial t}\overline{u_i u_j\theta} = -\frac{\partial}{\partial z}\overline{u_i u_j w\theta} + \overline{u_i u_j}\frac{\partial\overline{w\theta}}{\partial z} + \overline{u_i\theta}\frac{\partial\overline{u_j w}}{\partial z} + \overline{u_j\theta}\frac{\partial\overline{u_i w}}{\partial z} + \beta\overline{u_i u_j w} - \frac{2c_8}{\tau}\overline{u_i u_j\theta} + \lambda(\overline{u_i\theta^2}\delta_{3j} + \overline{u_j\theta^2}\delta_{3i}), \tag{4b}$$

$$\frac{\partial}{\partial t}\overline{u_i\theta^2} = -\frac{\partial}{\partial z}\overline{u_i w\theta^2} + 2\overline{u_i\theta}\frac{\partial\overline{w\theta}}{\partial z} + \overline{\theta^2}\frac{\partial\overline{u_i w}}{\partial z} + 2\beta\overline{u_i w\theta} - \frac{2c_8}{\tau}\overline{u_i\theta^2} + \lambda\overline{\theta^3}\delta_{3i}, \tag{4c}$$

$$\frac{\partial}{\partial t}\overline{\theta^3} = -\frac{\partial\overline{w\theta^3}}{\partial z} + 3\overline{\theta^2}\frac{\partial\overline{w\theta}}{\partial z} + 3\beta\overline{w\theta^2} - \frac{2c_{10}}{\tau}\overline{\theta^3}, \tag{4d}$$

where

$$\beta \equiv -\frac{\partial T}{\partial z}, \quad \lambda \equiv (1 - c_{11})g\alpha. \tag{4e}$$

To solve (4a)–(4d) for the TOMs, one needs expressions for the FOMs.

4. FOMs: Previous models

Most previous FOM models employed the quasi-normal (QN) approximation (see, e.g., Tatsumi 1957; O'Brien and Francis 1962; Ogura 1962; Zeman and Lumley 1976; André et al. 1976, 1978; Bougeault 1981; Chen and Cotton 1983; Moeng and Randall 1984; Canuto et al. 1994, 2001):

$$\begin{aligned}
&\overline{w^4}\big|_{\mathrm{QN}} = 3\overline{w^2}^2, && \overline{w^3\theta}\big|_{\mathrm{QN}} = 3\overline{w^2}\,\overline{w\theta},\\
&\overline{w^2\theta^2}\big|_{\mathrm{QN}} = \overline{w^2}\,\overline{\theta^2} + 2\overline{w\theta}^2, && \overline{w\theta^3}\big|_{\mathrm{QN}} = 3\overline{w\theta}\,\overline{\theta^2},\\
&\overline{u^2w^2}\big|_{\mathrm{QN}} = \overline{u^2}\,\overline{w^2}, && \overline{u^2w\theta}\big|_{\mathrm{QN}} = \overline{u^2}\,\overline{w\theta}.
\end{aligned} \tag{5a}$$

Using (5a), we have solved (4a)–(4d) for the TOMs in the PBL under stationary conditions. The algebraic solutions for $\overline{w^3}$, $\overline{w^2\theta}$, $\overline{w\theta^2}$, and $\overline{\theta^3}$ contain a common denominator D_1, while the algebraic solutions for $\overline{u^2w}$ and $\overline{u^2\theta}$ contain a common denominator D_2:

$$D_1 = 9(1 - c_{11})^2x^2 - 4c_8(3c_8 + 7c_{10})(1 - c_{11})x + 16c_8^3c_{10},$$

$$D_2 = 4c_8^2 - (1 - c_{11})x, \tag{5b}$$

where:

$$x \equiv \tau^2 g\alpha\beta. \tag{5c}$$

The details of the numerators are unimportant for this discussion. In the unstable case ($\beta > 0$), D_1 may become zero at some critical value of $x \sim 20$ and D_2 may become zero at some larger value of x. The critical value ($\sim$20) is easily reachable in the convective PBL. Close to the critical value the TOMs grow explosively and violate the realizability condition derived from Schwarz's generalized inequalities (André et al. 1976):

$$|\overline{abc}| \le \min\left\{\begin{array}{l}[\overline{a^2}(\overline{b^2}\,\overline{c^2} + \overline{bc}^2)]^{(1/2)}\\ [\overline{b^2}(\overline{a^2}\,\overline{c^2} + \overline{ac}^2)]^{(1/2)}\\ [\overline{c^2}(\overline{a^2}\,\overline{b^2} + \overline{ab}^2)]^{(1/2)}\end{array}\right\}, \tag{5d}$$

where *a, b,* and *c* stand for any of *u*, *w*, and θ. To prevent this from happening, Canuto et al. (2001) proposed an ad hoc procedure to limit the value of x in the unstable case; as a result, the eddy sizes are chopped down and thus the transport is weakened. In the stable case ($\beta < 0$), Moeng and Randall (1984) pointed out that Eqs. (4a), (4b) under QN lead to a "wave equation":

$$\frac{\partial^2}{\partial t^2}\overline{w^3} = 3\lambda\beta\overline{w^3} + \text{other terms} \tag{5e}$$

with an oscillation frequency given by

$$f = (-3\lambda\beta)^{1/2}. \tag{5f}$$

This occurs in the upper part of the convective PBL. Similar wave equations resulted from other TOM equations. The oscillations generated by these wave equations occur in the numerical simulations but are not observed in the PBL and thus are spurious.

Although it is well known that the use of the QN for the FOMs can cause erratic growth or oscillation of the TOMs, not much detailed analysis has been made in the context of turbulence modeling in the PBL.

5. FOMs: New nonlocal model

In the present study we propose a new model for the FOMs. Since the QN (zero cumulants) of the FOMs causes singular behaviors of the TOMs, the new FOMs must include nonzero cumulants. In principle, to formulate a new FOM model one should start with the dynamic equations of the FOMs, but this would bring about a new set of parameterizations for the pressure and dissipation terms, and most of all, the need to model the fifth-order moments. Here, we propose a new and simpler approach. Using as an input the LES data for the TOMs and SOMs, we derive information about the fourth-order cumulants.

To proceed, we first rewrite Eqs. (4a)–(4d) by subtracting from both sides the z derivatives of the QN expressions (5a). Assuming stationarity and rearranging terms, we obtain the following:

$$\frac{\partial}{\partial z}\left(\overline{w^4} - \overline{w^4}\big|_{\rm QN}\right) = -2c_8\frac{\overline{w^3}}{\tau} + 3\lambda\overline{w^2\theta} - 3\overline{w^2}\frac{\partial}{\partial z}\overline{w^2} \tag{6a}$$

$$\frac{\partial}{\partial z}\left(\overline{w^3\theta} - \overline{w^3\theta}\big|_{\rm QN}\right) = -2c_8\frac{\overline{w^2\theta}}{\tau} + \beta\overline{w^3} + 2\lambda\overline{w\theta^2} - 2\overline{w^2}\frac{\partial}{\partial z}\overline{w\theta} - \overline{w\theta}\frac{\partial}{\partial z}\overline{w^2} \tag{6b}$$

$$\frac{\partial}{\partial z}\left(\overline{w^2\theta^2} - \overline{w^2\theta^2}\big|_{\rm QN}\right) = -2c_8\frac{\overline{w\theta^2}}{\tau} + 2\beta\overline{w^2\theta} + \lambda\overline{\theta^3} - \overline{w^2}\frac{\partial}{\partial z}\overline{\theta^2} - 2\overline{w\theta}\frac{\partial}{\partial z}\overline{w\theta} \tag{6c}$$

$$\frac{\partial}{\partial z}\left(\overline{w\theta^3} - \overline{w\theta^3}\big|_{\rm QN}\right) = -2c_{10}\frac{\overline{\theta^3}}{\tau} + 3\beta\overline{w\theta^2} - 3\overline{w\theta}\frac{\partial}{\partial z}\overline{\theta^2} \tag{6d}$$

$$\frac{\partial}{\partial z}\left(\overline{u^2w^2} - \overline{u^2w^2}\big|_{\rm QN}\right) = -2c_8\frac{\overline{u^2w}}{\tau} + \lambda\overline{u^2\theta} - \overline{w^2}\frac{\partial}{\partial z}\overline{u^2} \tag{6e}$$

$$\frac{\partial}{\partial z}\left(\overline{u^2w\theta} - \overline{u^2w\theta}\big|_{\rm QN}\right) = -2c_8\frac{\overline{u^2\theta}}{\tau} + \beta\overline{u^2w} - \overline{w\theta}\frac{\partial}{\partial z}\overline{u^2}. \tag{6f}$$

In (6a)–(6f), the lhs represent the z derivatives of the cumulants that we will parameterize as follows. We assume that the z derivatives of the cumulants can be approximated by appropriate linear combinations of the TOMs. This assumption assures that in the Gaussian limit, where the TOMs vanish, the FOMs become QN. We suggest the following expressions:

$$\frac{\partial}{\partial z}\left(\overline{w^4} - \overline{w^4}\big|_{\rm QN}\right) = p_1\frac{\overline{w^3}}{\tau} \tag{7a}$$

$$\frac{\partial}{\partial z}\left(\overline{w^3\theta} - \overline{w^3\theta}\big|_{\rm QN}\right) = p_2\frac{\overline{w^2\theta}}{\tau} + d_1\beta\overline{w^3} \tag{7b}$$

$$\frac{\partial}{\partial z}\left(\overline{w^2\theta^2} - \overline{w^2\theta^2}\big|_{\rm QN}\right) = p_3\frac{\overline{w\theta^2}}{\tau} + d_2\beta\overline{w^2\theta} \tag{7c}$$

TABLE 1. Constants for the non-Gaussian FOM model.

p_1	p_2	p_3	p_4	p_5	p_6	d_1	d_2	d_3	d_4
4	4	2	1	0	0	1	2	3	1

$$\frac{\partial}{\partial z}\left(\overline{w\theta^3} - \overline{w\theta^3}\big|_{\mathrm{QN}}\right) = p_4\frac{\overline{\theta^3}}{\tau} + d_3\beta\overline{w\theta^2} \tag{7d}$$

$$\frac{\partial}{\partial z}\left(\overline{u^2w^2} - \overline{u^2w^2}\big|_{\mathrm{QN}}\right) = p_5\frac{\overline{u^2w}}{\tau} \tag{7e}$$

$$\frac{\partial}{\partial z}\left(\overline{u^2w\theta} - \overline{u^2w\theta}\big|_{\mathrm{QN}}\right) = p_6\frac{\overline{u^2\theta}}{\tau} + d_4\beta\overline{u^2w}. \tag{7f}$$

The p and d constant values are then chosen so that (7a)–(7f) best match the full expressions (6a)–(6f) using as input the steady-state LES data for the TOMs and SOMs by Mironov et al. (2000). This simulates a convective PBL with 1-km top height and 50-m grid spacing, a resolution sufficiently high for the purpose of examining steady-state budgets of the closure model, and provides SOM and TOM statistics of the resolved scales (section 2b of Gryanik and Hartmann 2002). We also used the aircraft data on the FOMs to further adjust these constants. The best values were chosen as whole numbers for simplicity and are listed in Table 1. To show to what extent the model (7a)–(7f) approximates the LES data for (6a)–(6f), the z derivatives of the cumulants are plotted in Fig. 1. The thick solid lines represent Eqs. (7a)–(7f), the thin solid lines represent Eqs. (6a)–(6f), and the dashed lines represent the Gryanik and Hartmann (2002) model; finally, the dotted lines represent the QN. All the z derivatives of the cumulants have been normalized with appropriate combinations of the PBL height h, the Deardorff velocity scale w_*, and the temperature scale θ_*:

$$w_* = \left(g\alpha h\overline{w\theta}\big|_{\mathrm{surf}}\right)^{1/3}, \quad w_*\theta_* = \overline{w\theta}\big|_{\mathrm{surf}}. \tag{7g}$$

Figure 1 shows that (7a)–(7f) is a better approximation than the others. It must be noted that the comparison between (6a)–(6f) and (7a)–(7f) is not as good below $z/h = 0.2$ or close to the PBL top, probably because the LES data for the TOMs only contain the resolved component and miss the subgrid component, which is increasingly important near the surface and the top. Although the LES subgrid component for the TOMs is not available, in the case of the SOMs, the subgrid component can be of the same order of magnitude as the resolved component for $z/h < 0.2$ and can overwhelm the resolved component for $z/h < 0.1$. An example is Fig. 18 of Moeng and Sullivan (1994), for PBLs driven by both shear and buoyancy, with grid spacing of 10 m. In general, coarse numerical resolution and the lack of a reliable subgrid model make the LES less accurate near the boundaries. Thus the comparison in those regions is not to be taken too seriously.

The new FOM model (7a)–(7f) can be rewritten as follows: New FOM model:

$$\overline{w^4} = \overline{w^4}\big|_{\mathrm{QN}} + p_1\int_0^z \frac{\overline{w^3}}{\tau}\,dz \tag{8a}$$

$$\overline{w^3\theta} = \overline{w^3\theta}\big|_{\mathrm{QN}} + \int_0^z \left(p_2\frac{\overline{w^2\theta}}{\tau} + d_1\beta\overline{w^3}\right)dz \tag{8b}$$

$$\overline{w^2\theta^2} = \overline{w^2\theta^2}\big|_{\mathrm{QN}} + \int_0^z \left(p_3\frac{\overline{w\theta^2}}{\tau} + d_2\beta\overline{w^2\theta}\right)dz \tag{8c}$$

$$\overline{w\theta^3} = \overline{w\theta^3}\big|_{\mathrm{QN}} + \int_0^z \left(p_4\frac{\overline{\theta^3}}{\tau} + d_3\beta\overline{w\theta^2}\right)dz \tag{8d}$$

$$\overline{u^2w^2} = \overline{u^2w^2}\big|_{\mathrm{QN}} + p_5\int_0^z \frac{\overline{u^2w}}{\tau}\,dz \tag{8e}$$

$$\overline{u^2w\theta} = \overline{u^2w\theta}\big|_{\mathrm{QN}} + \int_0^z \left(p_6\frac{\overline{u^2\theta}}{\tau} + d_4\beta\overline{u^2w}\right)dz, \tag{8f}$$

which highlights the nonlocal nature of the FOM closure model. The choice of the constants p in Table 1 effectively modifies the coefficients of the slow terms in the TOM equations, and thus helps provide adequate damping that was lacking in previous models. In addition, the choice of the constants d in Table 1 makes the z derivatives of the cumulants cancel out the β terms in the TOM equations, as will be shown in (9a)–(9f). Zeman and Lumley (1976), assuming zero cumulants, neglected β terms in (4b), (4c) arguing that they are small, while keeping the similar term in (4d). Here we argue that the β terms in (4b), (4c), and (4d) are canceled out by the nonzero cumulants. This argument is supported by the TOM equations and the LES data as presented in Fig. 1. For example, Fig. 1f shows that the lhs of (6f) can be replaced by the rhs of (7f), thus the β terms cancel in (6f). In addition, the cancellation of the β terms in (4b)–(4d) not only greatly simplifies the TOM equations, but also avoids the singularities in the unstable case and eliminates the source of the spurious oscillations in the stable case. Thus, in the following formulae, we will insert the values of the d's in Table 1, while retaining the p's as parameters since they may be further tuned when more data become available.

To assess the validity of the new FOM model, we compare (8a)–(8f) with the measured data by plotting the modeled FOMs with the SOMs and TOMs from the LES data (Mironov et al. 2000) as input, versus z/h (h is the PBL height). In Fig. 2, the thick solid lines represent the new model results, the filled circles represent the aircraft data of Hartmann et al. (1999), the dashed and dotted lines represent the model results of Gryanik and Hartmann (2002) and QN, respectively.

The kurtosis of w from the models and from the aircraft data is plotted in Fig. 2e. Our model results as shown in the figure coincide with the measurements of

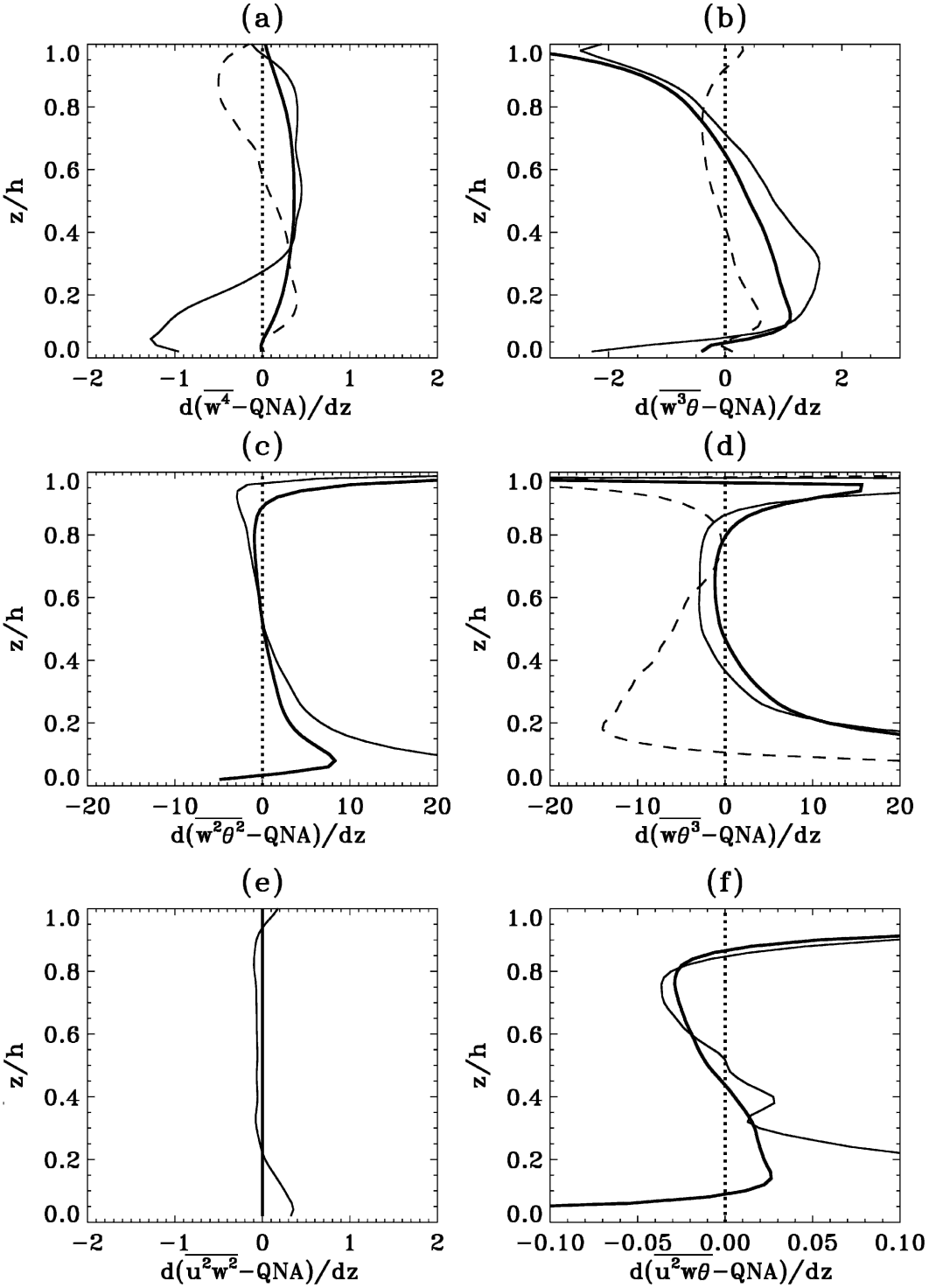

FIG. 1. Normalized z derivatives of the fourth-order cumulants vs the normalized height z/h in a convective PBL, using the LES data of Mironov et al. (2000) for lower-order moments as input. The thick solid lines represent results from the present FOM model (7a)–(7f), the thin solid lines represent results from the TOM budget Eqs. (6a)–(6f), the dashed lines represent the model of Gryanik and Hartmann (2002), and the dotted lines represent the QN (zero valued).

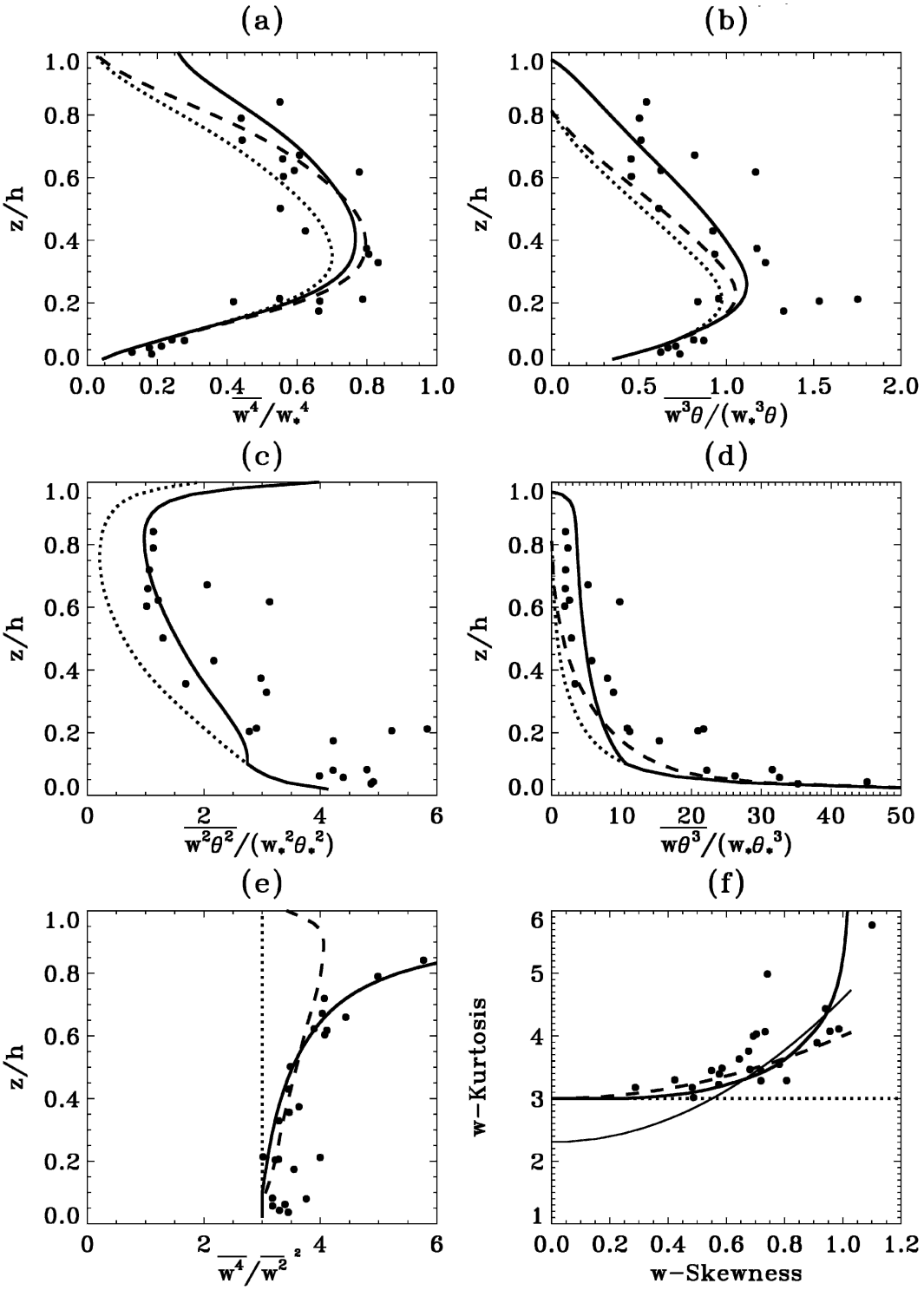

FIG. 2. (a)–(d) The normalized FOMs are plotted vs z/h in a convective PBL, using the LES data of Mironov et al. (2000) for lower-order moments as input. The solid lines represent results from the present model (8a)–(8f), the dashed lines represent results from the recent model of Gryanik and Hartmann (2002), and the dotted lines represent the QN. The filled circles are the aircraft data of Hartmann et al. (1999). (e) The kurtosis of w is plotted vs z/h. The thick solid line represents the result from the new model, the dashed line represents the result from the model of Gryanik and Hartmann (2002), and the dotted line represents the QN; for comparison the aircraft data are the filled circles. (f) The w-kurtosis K_w is plotted vs w-skewness S_w, using the new model (thick solid line), the model of Gryanik and Hartmann (2002; dashed line), and the QN (dotted line); for comparison the aircraft data are the filled circles, and the empirical formula $K_w = 2.3\ (S_w^2 + 1)$ is the thin solid line.

w kurtosis by Lenschow et al. (1994, 2000) who stated that "the kurtosis increases with height from around 3 to about 5 near 0.9 z/z_i. . . . Above $0.9z/z_i$ the kurtosis increases sharply".

In Fig. 2f we plot the w-kurtosis K_w versus skewness S_w from the new model (thick solid line) and from Gryanik and Hartmann (2002; dashed line) to be compared with the aircraft data (filled circles), and with the empirical formula (Alberghi et al. 2002; thin solid line):

$$K_w = 2.3(S_w^2 + 1). \tag{8g}$$

For the purpose of comparing the model with the FOM data, we assume that near the surface the cumulants, the integrals in (8a)–(8f), are small so that we can neglect them (i.e., assume QN) for $z/h < 0.1$ and reset the lower limits of these integrals to 0.1h for $z/h \geq 0.1$. With this approximation, in plotting Fig. 2 the spurious contributions due to the inaccurate LES data near the surface can be excluded, and in the PBL simulations, the sensitivities related to the boundary conditions are reduced. Judging from the comparisons with these data, the new model exhibits significant improvements as compared with QN and the Gryanik and Hartmann (2002) model. The FOM $\overline{\theta^4}$ is not directly needed in the present TOM model.

The nonlocality of Eqs. (8a)–(8f) is worth additional comment. Figure 2e shows that near the PBL top while the skewness S_w approaches zero, the kurtosis K_w does not approach the Gaussian value of 3, in fact, it continues to increase with height, in consistency with Lenschow et al. (1994, 2000)'s measurements. A local expansion of FOMs in terms of TOMs, as done by previous authors, such as Gryanik and Hartmann (2002), that yields $K_w = 3 + S_w^2$, cannot account for this feature. Our suggestion is that the relation between TOMs and FOMs must be nonlocal, so, for example, the value of $\overline{w^4}$ at a given height z depends not only on the value of $\overline{w^3}$ at that z (which may be small) but more generally on the values of $\overline{w^3}$ at other z's. Such nonlocal relations between TOMs and FOMs are expressed by Eqs. (8a)–(8f).

6. New TOM model with new FOMs

Next, we employ the new FOM expressions (8a)–(8f) in the TOM Eqs. (4a)–(4d), with the values of d's as specified in Table 1, but leaving p's as free parameters. The resulting equations are simpler than in previous models and more importantly, they are singularity-free. The full equations are as follows:

New prognostic TOM model:

$$\frac{\partial}{\partial t}\overline{w^3} = -(2c_8 + p_1)\frac{\overline{w^3}}{\tau} + 3\lambda\overline{w^2\theta} - 3\overline{w^2}\frac{\partial}{\partial z}\overline{w^2} \tag{9a}$$

$$\frac{\partial}{\partial t}\overline{w^2\theta} = -(2c_8 + p_2)\frac{\overline{w^2\theta}}{\tau} + 2\lambda\overline{w\theta^2} - 2\overline{w^2}\frac{\partial}{\partial z}\overline{w\theta} - \overline{w\theta}\frac{\partial}{\partial z}\overline{w^2} \tag{9b}$$

$$\frac{\partial}{\partial t}\overline{w\theta^2} = -(2c_8 + p_3)\frac{\overline{w\theta^2}}{\tau} + \lambda\overline{\theta^3} - \overline{w^2}\frac{\partial}{\partial z}\overline{\theta^2} - 2\overline{w\theta}\frac{\partial}{\partial z}\overline{w\theta} \tag{9c}$$

$$\frac{\partial}{\partial t}\overline{\theta^3} = -(2c_{10} + p_4)\frac{\overline{\theta^3}}{\tau} - 3\overline{w\theta}\frac{\partial}{\partial z}\overline{\theta^2} \tag{9d}$$

$$\frac{\partial}{\partial t}\overline{u^2w} = -(2c_8 + p_5)\frac{\overline{u^2w}}{\tau} + \lambda\overline{u^2\theta} - \overline{w^2}\frac{\partial}{\partial z}\overline{u^2} \tag{9e}$$

$$\frac{\partial}{\partial t}\overline{u^2\theta} = -(2c_8 + p_6)\frac{\overline{u^2\theta}}{\tau} - \overline{w\theta}\frac{\partial}{\partial z}\overline{u^2}. \tag{9f}$$

Equations (9a)–(9f) can be integrated in time. Alternatively, we present the stationary solution of (9a)–(9f), which is algebraic and explicit:

New algebraic TOM model:

$$\overline{w^3} = -A_1\frac{\partial}{\partial z}\overline{w^2} - A_2\frac{\partial}{\partial z}\overline{w\theta} - A_3\frac{\partial}{\partial z}\overline{\theta^2} \tag{10a}$$

$$\overline{w^2\theta} = -A_4\frac{\partial}{\partial z}\overline{w^2} - A_5\frac{\partial}{\partial z}\overline{w\theta} - A_6\frac{\partial}{\partial z}\overline{\theta^2} \tag{10b}$$

$$\overline{w\theta^2} = -A_7\frac{\partial}{\partial z}\overline{w\theta} - A_8\frac{\partial}{\partial z}\overline{\theta^2} \tag{10c}$$

$$\overline{\theta^3} = -A_9\frac{\partial}{\partial z}\overline{\theta^2} \tag{10d}$$

$$\overline{u^2w} = -A_{10}\frac{\partial\overline{u^2}}{\partial z} \tag{10e}$$

$$\overline{u^2\theta} = -A_{11}\frac{\partial\overline{u^2}}{\partial z}. \tag{10f}$$

All the resulting TOM expressions exhibit the structure of a linear combination of the z derivatives of the SOMs first discussed in Canuto et al. (1994, 2001). In (10a)–(10f), the diffusivities A's are given by:

$$A_1 = (a_1\overline{w^2} + a_2\lambda\tau\overline{w\theta})\tau, \qquad A_2 = (a_3\overline{w^2} + a_4\lambda\tau\overline{w\theta})\lambda\tau^2,$$
$$A_3 = (a_5\overline{w^2} + a_6\lambda\tau\overline{w\theta})\lambda^2\tau^3, \quad A_4 = a_7\tau\overline{w\theta},$$
$$A_5 = (a_8\overline{w^2} + a_9\lambda\tau\overline{w\theta})\tau, \qquad A_6 = (a_{10}\overline{w^2} + a_{11}\lambda\tau\overline{w\theta})\lambda\tau^2,$$
$$A_7 = a_{12}\tau\overline{w\theta}, \qquad A_8 = (a_{13}\overline{w^2} + a_{14}\lambda\tau\overline{w\theta})\tau,$$
$$A_9 = a_{15}\tau\overline{w\theta}, \qquad A_{10} = (a_{16}\overline{w^2} + a_{17}\lambda\tau\overline{w\theta})\tau,$$
$$A_{11} = a_{18}\tau\overline{w\theta}. \tag{11}$$

TABLE 2. Constants for the TOM and SOM models.

c_2	c_4	c_5	c_6	c_7	c_8	c_{10}	c_{11}
1	1.75	0.3	3.25	0.5	5	5	0.1

The coefficients a's in (11) are constants that can be derived from the basic constants c_8, c_{10}, c_{11}, and the p's as given in appendix C. Their values are listed in Tables 1–3.

There are several new features of the new TOM expressions (10a)–(10f) worth noting. In the unstable case, they are free of the singularity problems discussed in section 4, because there are no denominators akin to (5b). In the stable case, the β terms, which appeared in the original equations and constituted the restoring force terms of the wave equations, have been cancelled out by the z derivatives of the nonzero cumulants, no wave equations are formed from (9a)–(9f) and thus the spurious oscillation discussed in section 4 are no longer present. Finally, both the TOM budget equations and the algebraic expressions are significantly simplified as compared with the earlier models using the QN (Canuto et al. 1994, 2001). The much greater stability gained from removing the dependence on β from the TOM equations was noticed by Kupka (1999).

7. PBL simulation

Using the present model we run a full numerical simulation for a convective PBL. The mean temperature Eq. (1) and the SOM Eqs. (2a)–(2d) were integrated in time to reach a quasi-stationary state. The TOMs appearing in (2a)–(2d) were calculated using the algebraic model (10a)–(10f); the latter have been obtained by using the new FOMs (8a)–(8f). The dissipation rate ε and the time scale τ are parameterized through the length scale ℓ:

$$\varepsilon = \frac{q^3}{B_1 \ell}, \quad \tau = \frac{B_1 \ell}{q}, \quad \frac{1}{\ell} = \frac{1}{\ell_0} + \frac{1}{\ell_S} + \frac{1}{\ell_B}, \tag{12a}$$

where $B_1 = 19.3$ (Cheng et al. 2002), $\ell_0 = 0.15h$ where h is the PBL height (Moeng and Randall 1984), while the surface length ℓ_S is according to Nakanishi (2001):

$$\ell_S = \begin{cases} \kappa z/3.7, & \zeta \geq 1 \\ \kappa z(1 + 2.7\zeta)^{-1}, & 0 \geq \zeta < 1 \\ \kappa z(1 - 100\zeta)^{0.2}, & \zeta < 0 \end{cases}. \tag{12c}$$

Here, $\kappa = 0.4$ is the von Kármán constant, $\zeta = z/L_M$ and $L_M = -u_*^3/(\kappa g \alpha \overline{w\theta}|_{\text{surf}})$ is the Obukhov length. However, for (12c) to work properly in the purely buoyancy-driven PBL where $L_M = 0$, we found it necessary to modify (12c); accordingly we took $\zeta = -5z/h$ instead.

TABLE 3. Derived constants calculated using Tables 1 and 2 and Eqs. (C1)–(C2).

a_1	2.1429×10^{-1}	a_7	7.1429×10^{-2}	a_{13}	8.3333×10^{-2}
a_2	1.5306×10^{-2}	a_8	1.4286×10^{-1}	a_{14}	2.2727×10^{-2}
a_3	3.0612×10^{-2}	a_9	2.3810×10^{-2}	a_{15}	2.7273×10^{-1}
a_4	5.1020×10^{-3}	a_{10}	1.1905×10^{-2}	a_{16}	1.0000×10^{-1}
a_5	2.5510×10^{-3}	a_{11}	3.2468×10^{-3}	a_{17}	1.0000×10^{-2}
a_6	6.9573×10^{-4}	a_{12}	1.6667×10^{-1}	a_{18}	1.0000×10^{-1}

The buoyancy length ℓ_B is according to Deardorff (1976) and André et al. (1978):

$$\ell_B = \begin{cases} \infty & \text{if } N^2 \leq 0 \\ 0.53q/N & \text{if } N^2 > 0 \end{cases}, \quad N^2 = g\alpha \frac{\partial T}{\partial z}. \tag{12d}$$

The initial and boundary conditions, as well as the numerical algorithm and grid spacing (corresponding to 33 m in a mixed layer with 1 km height) are the same as those in Canuto et al. (1994); the model constants used are listed in Tables 1–3. In a separate sensitivity test run we doubled the grid spacing (without making any other changes) and found that the results were almost the same. The results for mean potential temperature T, several SOMs, ε, ε_θ, and several TOMs are presented in Figs. 3–4 where the solid lines correspond to the new model results, and dot–dashed lines are the LES data of Mironov et al. (2000) and the filled circles are the aircraft data of Hartmann et al. (1999). All the turbulent quantities have been normalized by appropriate combinations of the PBL height, h, the Deardorff velocity scale, w_*, and the temperature scale, θ_*. The new model shows improvements as compared with the similar PBL simulation of Canuto et al. (1994); in particular, the TOMs are damped more properly using the new model and the clipping approximation (5d) is no longer needed in the current simulation.

To further verify the new FOM model, we substitute the SOMs and TOMs obtained from the PBL simulation into the new FOM model (8a)–(8f) and plot in Fig. 5 the resulting FOMs (solid lines) and the QN results (dotted lines) in comparison with the aircraft data (filled circles). The TOMs presented have been normalized by w_* and θ_*. The new model compares well with the data, indicating internal consistency. The PBL code with the new TOMs runs twice as fast as with the previous TOM model of Canuto et al. (1994).

8. Conclusions

While local turbulence models severely underestimate the turbulent transport in the convective PBL, previous nonlocal models, most of which employ the quasi-normal approximation, have their own problems. The quasi-normal approximation fails to provide appropriate damping of the TOMs in both the stable and the unstable cases, causing singular or oscillating behavior in the PBL. The clipping approximation relieved the problem but the damping is minimal and not suffi-

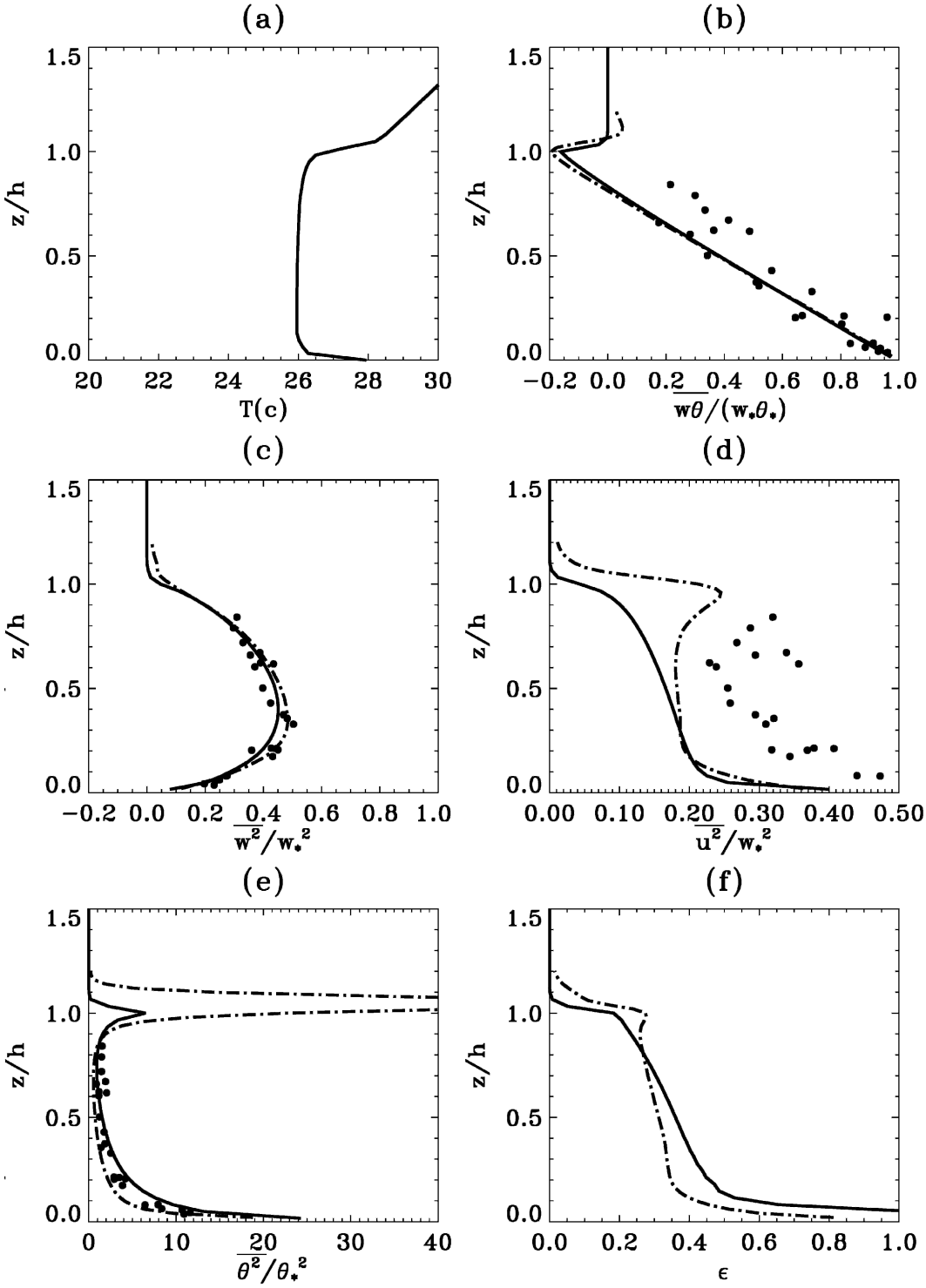

FIG. 3. Mean potential temperature T, normalized SOMs, and ε vs z/h resulting from a numerical simulation of a convective PBL described in section 7; ε has been normalized by w_*^3/h. The solid lines represent the new model, the dot–dashed lines represent the LES data of Mironov et al. (2000), and the filled circles represent the aircraft data of Hartmann et al. (1999). In (d), the larger values of $\overline{u^2}$ in the aircraft data are due to the nonzero wind condition, while the LES used was made under zero mean wind condition, resulting in smaller values of $\overline{u^2}$ [see section 2c of Gryanik and Hartmann (2002) for details].

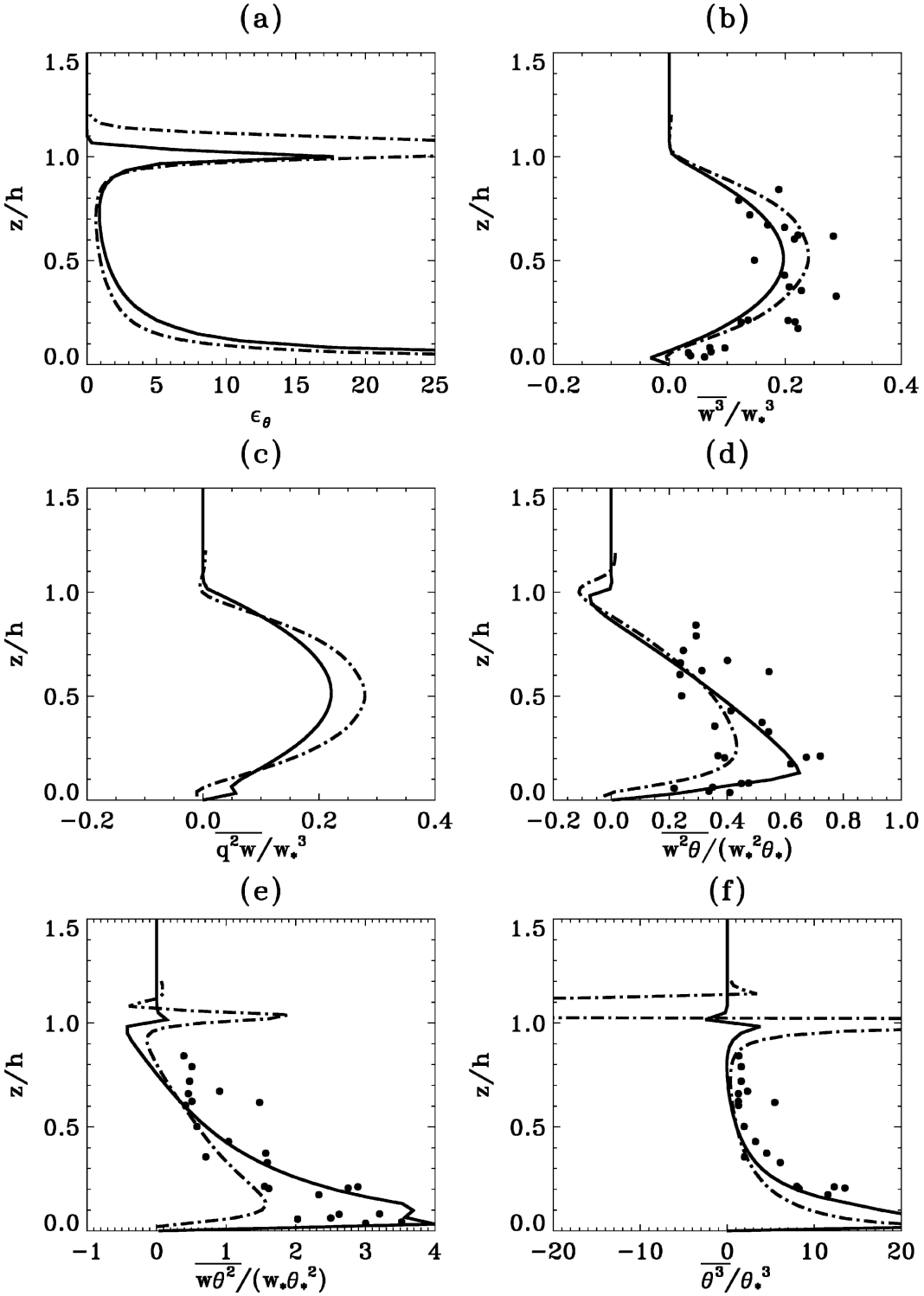

FIG. 4. Same as Fig. 3 but for normalized ε_θ and TOMs; ε_θ has been normalized by $w_*\theta_*^2/h$.

cient. Adding a diffusion term lacks theoretical basis and the results are sensitive to the arbitrary coefficient. In addition, previous models derived from the dynamic equations were quite complex.

In this study we have addressed the above issues. We started by modifying a popular parameterization of the pressure correlation in the TOM equations to ensure the realizability conservation. We then parameterized

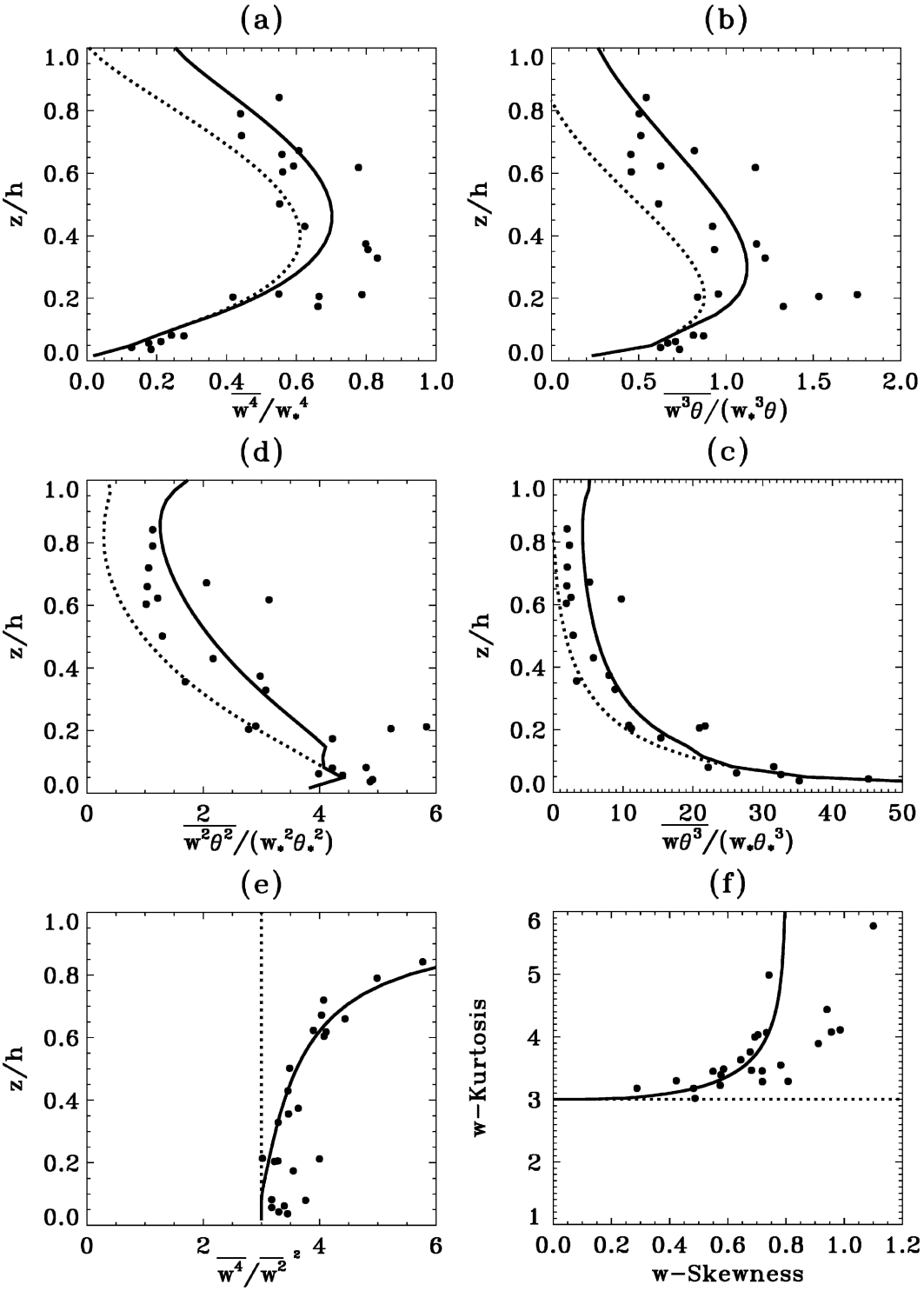

FIG. 5. Normalized FOMs vs z/h according to the FOM model (8a)–(8f), as solid lines, using T, SOMs, and TOMs resulting from the numerical simulation of a convective PBL as input, with QN FOMs as dotted lines. The filled circles represent the aircraft data of Hartmann et al. (1999).

the fourth-order cumulants by analyzing the balanced TOM equations, aided by the LES data for TOMs and SOMs. The new TOM model is based on the new FOMs and improved pressure correlations.

The new, non-Gaussian FOMs seem to provide appropriate damping to the TOMs: in the unstable region, which corresponds to the lower part of the convective PBL, the TOM expressions are now free of the singularity that caused the TOM to diverge; in the stable region, which corresponds to the upper part of the convective PBL, the source of the reported spurious oscillation is canceled out by part of the nonzero cumulants in the new FOMs.

Numerical simulation of a convective PBL was performed using the new model, yielding results that compare well with the LES and measured aircraft data. The new FOM model was then further verified by substituting back the SOMs and TOMs from the PBL simulation. A natural extension of the present study is to include the shear effects in the FOM and TOM models and that shall be considered as a future research topic.

Acknowledgments. We thank Drs. V. M. Gryanik, J. Hartmann, D. V. Mironov, and F. Kupka for kindly providing us with the LES and aircraft data and for useful discussions.

APPENDIX A

SOMs: Nonlocal Model

To facilitate the discussion, we list the dynamic, second-order closure equations in the convective PBL (see, e.g., Canuto 1992).

Mean potential temperature T:

$$\frac{\partial T}{\partial t} = -\frac{\partial}{\partial z}\overline{w\theta}, \tag{A1}$$

where w and θ are the fluctuating parts of the vertical component of the velocity and the potential temperature, respectively, and $\overline{w\theta}$ is the vertical component of the heat flux $\overline{u_i\theta}$. Heat flux $\overline{u_i\theta}$:

$$\frac{\partial}{\partial t}\overline{u_i\theta} = -D_i^{\theta} - \overline{u_i w}\frac{\partial T}{\partial z} + g\alpha\overline{\theta^2}\delta_{3i} - \Pi_i^{\theta}, \tag{A2}$$

where g is the gravitational acceleration, α is the coefficient of thermal expansion, D_i^{θ} is the TOM term, and Π_i^{θ} is the pressure–temperature correlation (to be defined below). Reynolds stresses $\overline{u_iu_j}$:

$$\frac{\partial}{\partial t}\overline{u_iu_j} = -D_{ij} + g\alpha(\overline{u_i\theta}\delta_{3j} + \overline{u_j\theta}\delta_{3i}) - \Pi_{ij} - \frac{2}{3}\varepsilon\delta_{ij}, \tag{A3}$$

where D_{ij} is the TOM term, Π_{ij} is the pressure–velocity correlation, and ε is the dissipation rate of turbulent kinetic energy:

$$K = \frac{1}{2}\overline{q^2}, \quad q^2 \equiv u_iu_i. \tag{A4}$$

Potential temperature variance $\overline{\theta^2}$:

$$\frac{\partial}{\partial t}\overline{\theta^2} = -D^{\theta\theta} - 2\overline{w\theta}\frac{\partial T}{\partial z} - 2\varepsilon_{\theta}, \tag{A5}$$

where $D^{\theta\theta}$ is the TOM term and ε_{θ} is the dissipation rate of $\overline{\theta^2}$. In the above equations, the TOM terms are defined as follows:

$$D_i^{\theta} \equiv \frac{\partial}{\partial z}\overline{u_iw\theta}, \quad D_{ij} \equiv \frac{\partial}{\partial z}\overline{u_iu_jw}, \quad D^{\theta\theta} \equiv \frac{\partial}{\partial z}\overline{w\theta^2}, \tag{A6}$$

while the pressure–correlations terms are defined as follows:

$$\rho_0\Pi_i^{\theta} \equiv \overline{\theta\frac{\partial p}{\partial x_i}}, \quad \rho_0\Pi_{ij} \equiv \overline{u_i\frac{\partial p}{\partial x_j}} + \overline{u_j\frac{\partial p}{\partial x_i}}, \tag{A7}$$

where ρ_0 is the reference density and p is the fluctuating part of the pressure. We adopt the following closure for the pressure correlations (Zeman and Lumley 1979; Canuto 1992):

$$\Pi_{ij} = \frac{2c_4}{\tau_p}\left(\overline{u_iu_j} - \frac{1}{3}\overline{q^2}\delta_{ij}\right) + c_5g\alpha\left(\overline{u_i\theta}\delta_{3j} + \overline{u_j\theta}\delta_{3i} - \frac{2}{3}\delta_{ij}\overline{w\theta}\right) \tag{A8}$$

$$\Pi_i^{\theta} = \frac{2c_6}{\tau_p}\overline{u_i\theta} + c_7g\alpha\overline{\theta^2}\delta_{3i}, \tag{A9}$$

and the dissipation rates are parameterized in terms of a dynamic time scale τ:

$$\varepsilon = \frac{\overline{q^2}}{\tau}, \quad \varepsilon_{\theta} = \frac{2c_2}{\tau}\overline{\theta^2}, \tag{A10}$$

τ_p is the return-to-isotropy time scale (Canuto et al. 1994):

$$\tau_p = \frac{\tau}{1 + C_wN^2\tau^2} \tag{A11}$$

$$N^2 = g\alpha\frac{\partial T}{\partial z}, \quad C_w = \begin{cases} 0 & \text{if } N^2 \le 0 \\ 0.04 & \text{if } N^2 > 0 \end{cases}, \tag{A12}$$

and c_2–c_7 are model constants, which are the same as in Canuto et al. (1994), are given in Table 2.

APPENDIX B

TOM Equations and Modified Closure for Π_{ij}^{θ}

Following André et al. (1982), the TOM equations are

$$\frac{\partial}{\partial t}\overline{u_iu_jw} = -D_{ij3} + \overline{u_iu_j}\frac{\partial\overline{w^2}}{\partial z} + \overline{u_jw}\frac{\partial\overline{u_iw}}{\partial z} + \overline{u_iw}\frac{\partial\overline{u_jw}}{\partial z} + g\alpha(\overline{u_iu_j\theta} + \overline{u_iw\theta}\delta_{3j} + \overline{u_jw\theta}\delta_{3i}) - \Pi_{ij3} - \varepsilon_{uuu} \quad \text{(B1)}$$

$$\frac{\partial}{\partial t}\overline{u_iu_j\theta} = -D^{\theta}_{ij} + \overline{u_iu_j}\frac{\partial\overline{w\theta}}{\partial z} + \overline{u_i\theta}\frac{\partial\overline{u_jw}}{\partial z} + \overline{u_j\theta}\frac{\partial\overline{u_iw}}{\partial z} - \overline{u_iu_jw}\frac{\partial T}{\partial z} + \alpha g(\overline{u_i\theta^2}\delta_{3j} + \overline{u_j\theta^2}\delta_{3i}) - \Pi^{\theta}_{ij} - \varepsilon_{uu\theta} \quad \text{(B2)}$$

$$\frac{\partial}{\partial t}\overline{u_i\theta^2} = -D^{\theta\theta}_{i} + 2\overline{u_i\theta}\frac{\partial\overline{w\theta}}{\partial z} + \overline{\theta^2}\frac{\partial\overline{u_iw}}{\partial z} - 2\overline{u_iw\theta}\frac{\partial T}{\partial z} + g\alpha\overline{\theta^3}\delta_{3i} - \Pi^{\theta\theta}_{i} - \varepsilon_{u\theta\theta} \quad \text{(B3)}$$

$$\frac{\partial}{\partial t}\overline{\theta^3} = -\frac{\partial\overline{w\theta^3}}{\partial z} + 3\overline{\theta^2}\frac{\partial\overline{w\theta}}{\partial z} - 3\overline{w\theta^2}\frac{\partial T}{\partial z} - \varepsilon_{\theta\theta\theta}, \quad \text{(B4)}$$

where D's are the FOM terms,

$$D_{ij3} \equiv \frac{\partial}{\partial z}\overline{u_iu_jw^2}, \quad D^{\theta}_{ij} \equiv \frac{\partial}{\partial z}\overline{u_iu_jw\theta}, \quad D^{\theta\theta}_{i} \equiv \frac{\partial}{\partial z}\overline{u_iw\theta^2}, \quad \text{(B5)}$$

and Π's are the pressure–correlations terms,

$$\rho_0\Pi_{ij3} \equiv \overline{u_iu_j\frac{\partial p}{\partial z}} + \overline{u_iw\frac{\partial p}{\partial x_j}} + \overline{u_jw\frac{\partial p}{\partial x_i}}, \quad \text{(B6)}$$

$$\rho_0\Pi^{\theta}_{ij} \equiv \overline{u_i\theta\frac{\partial p}{\partial x_j}} + \overline{u_j\theta\frac{\partial p}{\partial x_i}}, \quad \rho_0\Pi^{\theta\theta}_{i} = \overline{\theta^2\frac{\partial p}{\partial x_i}}, \quad \text{(B7)}$$

while ε's are the dissipation rates. Following André et al. (1982), use of the isotropy at the dissipation scales gives:

$$\varepsilon_{uuu} = \varepsilon_{u\theta\theta} = 0, \quad \varepsilon_{uu\theta} = \frac{2c_{10}}{3\tau}\delta_{ij}\overline{u_ku_k\theta}, \quad \varepsilon_{\theta\theta\theta} = \frac{2c_{10}}{\tau}\overline{\theta^3}, \quad \text{(B8)}$$

where c_{10} is a model constant. The pressure correlation terms are parameterized with a return-to-isotropy part and a fast part; the main reason for the introduction of the latter is to damp the triple correlations. We have

$$\Pi_{ij3} = \frac{2c_8}{\tau}\overline{u_iu_jw} + c_{11}g\alpha(\overline{u_iu_j\theta} + \overline{u_iw\theta}\delta_{3j} + \overline{u_jw\theta}\delta_{3i}) \quad \text{(B9)}$$

$$\Pi^{\theta\theta}_{i} = \frac{2c_8}{\tau}\overline{u_i\theta^2} + c_{11}g\alpha\overline{\theta^3}\delta_{3i}, \quad \text{(B10)}$$

where c_8 and c_{11} are model constants.

The parameterization of Π^{θ}_{ij}, which appears in (B2), has been difficult, as pointed out by André et al. (1982). The widely used closure for the correlation Π^{θ}_{ij}

$$\Pi^{\theta}_{ij} = \frac{2c_8}{\tau}\left(\overline{u_iu_j\theta} - \frac{1}{3}\delta_{ij}\overline{u_ku_k\theta}\right) + c_{11}g\alpha\left(\overline{u_i\theta^2}\delta_{3j} + \overline{u_j\theta^2}\delta_{3i} - \frac{2}{3}\delta_{ij}\overline{w\theta^2}\right) - \frac{2c_9}{\tau}\delta_{ij}\overline{u_ku_k\theta} \quad \text{(B11)}$$

is not consistent with realizability conservation, since it does not ensure that $\partial\overline{u^2\theta}/\partial t = 0$ whenever $u = 0$ (u is the x component of the fluctuating part of the velocity). To see this, using (B5), (B8), and (B11) in (B2) with $i = j = 1$ one obtains

$$\frac{\partial}{\partial t}\overline{u^2\theta} = -\frac{\partial}{\partial z}\overline{u^2w\theta} + \overline{u^2}\frac{\partial\overline{w\theta}}{\partial z} - \overline{u^2w}\frac{\partial T}{\partial z} - \frac{2c_8}{\tau}\overline{u^2\theta} + \left(c_9 + \frac{c_8}{3} - \frac{c_{10}}{3}\right)\frac{2}{\tau}\overline{u^2\theta} + \frac{2}{3}c_{11}\alpha g\overline{w\theta^2}. \quad \text{(B12)}$$

Although the parenthesis $[c_9 + (c_8/3) - (c_{10}/3)]$ in (B12) has been taken as zero (André et al. 1982), the rhs still does not vanish when u vanishes because of the presence of the last term, this behavior is unphysical and may cause problems in the numerical simulations of the boundary layer. We have reviewed the parameterization process and propose a remedy to the situation, such that Π^{θ}_{ij} is first divided into two parts (we have dropped ρ_0 for simplicity):

$$\Pi^{\theta}_{ij} \equiv \overline{u_i\theta\partial p/\partial x_j} + \overline{u_j\theta\partial p/\partial x_i} = (\partial\overline{u_i\theta p}/\partial x_j + \partial\overline{u_j\theta p}/\partial x_i) - (\overline{p\partial u_i\theta/\partial x_j} + \overline{p\partial u_j\theta/\partial x_i}). \quad \text{(B13)}$$

On the rhs of (B13), the first parenthesis is the transport or diffusion part and can be neglected or modeled together with the fourth moment terms, for example, for $i = j = 3$:

$$\frac{\partial}{\partial t}\overline{w^2\theta} = -\frac{\partial}{\partial z}(\overline{w^3\theta} + 2\overline{w\theta p}) + \text{other terms} \approx -\frac{\partial}{\partial z}(a\overline{w^3\theta}) + \text{other terms}, \quad \text{(B14)}$$

where a is a parameter close to 1. The second parenthesis on the rhs of (B13) can be further split into a traceless part and a diagonal part and then separately parameterized as follows:

$$-(\overline{p\partial u_i\theta/\partial x_j} + \overline{p\partial u_j\theta/\partial x_i}) = A + B, \quad \text{(B15)}$$

where

$$A \equiv -\left(\overline{p\partial u_i\theta/\partial x_j} + \overline{p\partial u_j\theta/\partial x_i} - \frac{2}{3}\delta_{ij}\overline{p\partial u_k\theta/\partial x_k}\right)$$
$$= \frac{2c_8}{\tau}\left(\overline{u_iu_j\theta} - \frac{1}{3}\delta_{ij}\overline{u_ku_k\theta}\right)$$
$$+ c_{11}g\alpha\left(\overline{u_i\theta^2}\delta_{3j} + \overline{u_j\theta^2}\delta_{3i} - \frac{2}{3}\delta_{ij}\overline{w\theta^2}\right) \quad \text{(B16)}$$

$$B \equiv -\frac{2}{3}\delta_{ij}\overline{p\partial u_k\theta/\partial x_k} = -\frac{2c_9}{\tau}\delta_{ij}\overline{u_ku_k\theta} + c_{12}\frac{2}{3}g\alpha\delta_{ij}\overline{w\theta^2}. \quad \text{(B17)}$$

In (B17) we have added the last term, which is new. Substituting (B5), (B8), and (B13), (B15)–(B17) in (B2) yields

$$\frac{\partial}{\partial t}\overline{u_iu_j\theta} = -\frac{\partial}{\partial z}\overline{u_iu_jw\theta} + \overline{u_iu_j}\frac{\partial\overline{w\theta}}{\partial z} + \overline{u_i\theta}\frac{\partial\overline{u_jw}}{\partial z}$$
$$+ \overline{u_j\theta}\frac{\partial\overline{u_iw}}{\partial z} - \overline{u_iu_jw}\frac{\partial T}{\partial z} - \frac{2c_8}{\tau}\overline{u_iu_j\theta}$$
$$+ (1 - c_{11})g\alpha(\overline{u_i\theta^2}\delta_{3j} + \overline{u_j\theta^2}\delta_{3i})$$
$$+ \left(c_9 + \frac{c_8}{3} - \frac{c_{10}}{3}\right)\frac{2}{\tau}\delta_{ij}\overline{u_ku_k\theta}$$
$$+ (c_{11} - c_{12})\frac{2}{3}g\alpha\delta_{ij}\overline{w\theta^2}. \quad \text{(B18)}$$

We suggest that both the parentheses in the last two terms in (B18) must be zero in order to ensure the realizability conservation, that is, $\partial\overline{u^2\theta}/\partial t = 0$ whenever $u = 0$.

APPENDIX C

Derived Constants for the New TOM Model (10a)–(10f)

The new algebraic TOM model in (10a)–(10f) and (11) contains some derived constants that can be calculated from the more basic model constants:

$$a_1 = \frac{3}{b_1}, \quad a_2 = \frac{3}{b_1b_2}, \quad a_3 = \frac{6}{b_1b_2}, \quad a_4 = \frac{12}{b_1b_2b_3},$$
$$a_5 = \frac{6}{b_1b_2b_3}, \quad a_6 = \frac{18}{b_1b_2b_3b_4}, \quad a_7 = \frac{1}{b_2}, \quad a_8 = \frac{2}{b_2},$$
$$a_9 = \frac{4}{b_2b_3}, \quad a_{10} = \frac{2}{b_2b_3}, \quad a_{11} = \frac{6}{b_2b_3b_4}, \quad a_{12} = \frac{2}{b_3},$$
$$a_{13} = \frac{1}{b_3}, \quad a_{14} = \frac{3}{b_3b_4}, \quad a_{15} = \frac{3}{b_4}, \quad a_{16} = \frac{1}{b_5},$$
$$a_{17} = \frac{1}{b_5b_6}, \quad a_{18} = \frac{1}{b_6}, \quad \text{(C1)}$$

where

$$b_i = 2c_8 + p_i \quad \textit{for } i = 1, 2, 3, 5, 6; \quad b_4 = 2c_{10} + p_4. \quad \text{(C2)}$$

We use the values for p's as listed in Table 1 and the basic model constants c_8, c_{10}, and c_{11} as listed in Table 2. The resulting values of the derived constants in (C1) are listed in Table 3.

REFERENCES

Alberghi, S., A. Maurizi, and F. Tampieri, 2002: Relationship between the vertical velocity skewness and kurtosis observed during sea-breeze convection. *J. Appl. Meteor.,* **41,** 885–889.

André, J. C., G. De Moor, P. Lacarrère, and R. du Vachat, 1976: Turbulence approximation for inhomogeneous flows: Part I. The clipping approximation. *J. Atmos. Sci.,* **33,** 476–481.

——, ——, ——, G. Therry, and R. du Vachat, 1978: Modeling the 24-hour evolution of the mean and turbulent structures of the planetary boundary layer. *J. Atmos. Sci.,* **35,** 1861–1883.

——, P. Lacarrére, and K. Traore, 1982: Pressure effects on triple correlations in turbulent convective flows. *Turbulent Shear Flows: Selected Papers from the Third International Symposium on Turbulent Shear Flows,* Vol. 3, L. J. S. Bradbury et al., Eds., Springer-Verlag, 243–252.

Bougeault, P., 1981: Modeling the trade-wind cumulus boundary layer. Part II: A high order one-dimensional model. *J. Atmos. Sci.,* **38,** 2429–2439.

Canuto, V. M., 1992: Turbulent convection with overshooting: Reynolds stress approach. *Astrophys. J.,* **392,** 218–232.

——, F. Minotti, C. Ronchi, R. M. Ypma, and O. Zeman, 1994: Second-order closure PBL model with new third-order moments: Comparison with LES data. *J. Atmos. Sci.,* **51,** 1605–1618.

——, Y. Cheng, and A. Howard, 2001: New third-order moments for the convective boundary layer. *J. Atmos. Sci.,* **58,** 1169–1172.

Chen, C., and W. R. Cotton, 1983: Numerical experiments with a one-dimensional high order turbulence model: Simulation of the Wangara Day 33 case. *Bound.-Layer Meteor.,* **25,** 375–404.

Cheng, Y., and V. M. Canuto, 1994: Stably stratified shear turbulence: A new model for the energy dissipation length scale. *J. Atmos. Sci.,* **51,** 2384–2396.

——, ——, and A. M. Howard, 2002: An improved model for the turbulent PBL. *J. Atmos. Sci.,* **59,** 1550–1565.

Deardorff, J. W., 1972: Theoretical expression for the countergradient vertical heat flux. *J. Geophys. Res.,* **77,** 5900–5904.

——, 1976: Clear and cloud-capped mixed layers: Their numerical simulation, structure and growth and parameterization. *Seminars on the Treatment of the Boundary Layer in Numerical Weather Prediction,* Bracknell, United Kingdom, European Centre for Medium-Range Weather Forecasts, 234–284.

——, 1978: Closure of second- and third-moment rate equations for diffusion in homogeneous turbulence. *Phys. Fluids,* **21,** 525–530.

Gryanik, V. M., and J. Hartmann, 2002: A turbulence closure for the convective boundary layer based on a two-scale mass-flux approach. *J. Atmos. Sci.,* **59,** 2729–2744.

Hartmann, J., and Coauthors, 1999: Arctic radiation and turbulence interaction study (ARTIST). Alfred Wegener Institute for Polar and Marine Research Rep. on Polar Research, No. 305, Bremerhaven, Germany, 81 pp.

Holtslag, A. A. M., and C.-H. Moeng, 1991: Eddy diffusivity and countergradient transport in the convective atmospheric boundary layer. *J. Atmos. Sci.,* **48,** 1690–1700.

——, and B. A. Boville, 1993: Local versus nonlocal boundary-layer diffusion in a global climate model. *J. Climate,* **6,** 1825–1842.

——, E. I. F. De Bruijn, and H.-L. Pan, 1990: A high resolution air mass transformation model for short-range weather forecasting. *Mon. Wea. Rev.,* **118,** 1561–1575.

Kantha, L. H., and C. A. Clayson, 1994: An improved mixed layer model for geophysical applications. *J. Geophys. Res.,* **99,** 25 235–25 266.

Kupka, F., 1999: Turbulent convection: Comparing the moment equations to numerical simulations. *Astrophys. J.,* **526,** L45–L48.

Lenschow, D. H., J. Mann, and L. Kristensen, 1994: How long is long enough when measuring fluxes and other turbulence statistics? *J. Atmos. Oceanic Technol.,* **11,** 661–673.

——, V. Wulfmeyer, and C. Senff, 2000: Measuring second-through fourth-order moments in noisy data. *J. Atmos. Oceanic Technol.,* **17,** 1330–1347.

Mellor, G. L., and T. Yamada, 1974: A hierarchy of turbulence closure models for planetary boundary layers. *J. Atmos. Sci.,* **31,** 1791–1806.

——, and ——, 1982: Development of a turbulence closure model for geophysical fluid problems. *Rev. Geophys. Space Phys.,* **20,** 851–875.

Mironov, D. V., V. M. Gryanik, C.-H. Moeng, D. J. Olbers, and T. H. Warncke, 2000: Vertical turbulence structure and second-moment budgets in convection with rotation: A large-eddy simulation study. *Quart. J. Roy. Meteor. Soc.*, **126,** 477–516.

Moeng, C.-H., and D. A. Randall, 1984: Problems in simulating the stratocumulus-topped boundary layer with a third-order closure model. *J. Atmos. Sci.,* **41,** 1588–1600.

——, and J. C. Wyngaard, 1989: Evaluation of turbulent transport and dissipation closures in second-order modeling. *J. Atmos. Sci.,* **46,** 2311–2330.

——, and P. P. Sullivan, 1994: A comparison of shear- and buoyancy-driven planetary boundary layer flows. *J. Atmos. Sci.,* **51,** 999–1022.

Nakanishi, M., 2001: Improvement of the Mellor-Yamada turbulence closure model based on large-eddy simulation data. *Bound.-Layer Meteor.,* **99,** 349–378.

O'Brien, E. E., and G. C. Francis, 1962: A consequence of the zero-fourth-cumulant approximation. *J. Fluid Mech.,* **13,** 369–375.

Ogura, Y., 1962: Energy transfer in isotropic turbulent flow. *J. Geophys. Res.,* **67,** 3143–3149.

Tatsumi, T., 1957: The theory of decay process of incompressible isotropic turbulence. *Proc. Roy. Soc. London,* **A239,** 16–45.

Troen, I., and L. Mahrt, 1986: A simple model of the atmospheric boundary layer: Sensitivity to surface evaporation. *Bound.-Layer Meteor.,* **37,** 129–148.

Wyngaard, J. C., and J. C. Weil, 1991: Transport asymmetry in skewed turbulence. *Phys. Fluids,* **A3,** 155–162.

Zeman, O., and J. L. Lumley, 1976: Modeling buoyancy driven mixed layers. *J. Atmos. Sci.,* **33,** 1974–1988.

——, and ——, 1979: Buoyancy effects in entraining turbulent boundary layers: A second-order closure study. *Turbulent Shear Flows: Selected Papers from the First International Symposium on Turbulent Shear Flows,* Vol. 1, F. Durst et al., Eds., Springer-Verlag, 295–306.

Zilitinkevich, S., V. M. Gryanik, V. N. Lykossov, and D. V. Mironov, 1999: Third-order transport and nonlocal turbulence closures for convective boundary layers. *J. Atmos. Sci.,* **56,** 3463–3477.